Internal Wave Tunnelling Through Non-uniformly Stratified Shear Flow

G. L. Brown[1] and B. R. Sutherland[2*]

[1]*Department of Earth and Atmospheric Sciences*
University of Alberta, Edmonton, Alberta
[2]*Department of Mathematical and Statistical Sciences*
University of Alberta, Edmonton, Alberta T6G 2G1

[Original manuscript received 18 April 2006; in revised form 13 October 2006]

ABSTRACT *We examine the transmission of internal gravity waves through a non-uniformly stratified fluid with vertically varying background shear. To quantify wave transmission we show that the appropriate measure is the ratio of the flux of transmitted to incident pseudoenergy, T. We derive an analytic prediction of T for the transmission of waves through a piecewise-linear shear flow in two cases. In both, the fluid is unstratified over the depth of the shear and uniformly stratified elsewhere.*

In one study, the density profile is continuous. Such a basic state is unstable but with vanishingly small growth rate as the bulk Richardson number, Ri, becomes large. In the limit of an infinitely large Richardson number (no shear), we recover the tunnelling prediction of Sutherland and Yewchuk (2004). In weak shear, incident waves can transmit weakly, even if the phase speed matches the flow speed within the shear layer (a critical level). However, no transmission occurs when the phase speed of incident waves exactly matches the flow speed on the opposite flank of the shear. In strong shear, with Ri ≃ 1, a transmission peak occurs where the incident wavenumber and frequency are close to, but different from, those associated with unstable modes.

In a second study, the background density profile is discontinuous and representative of a well-mixed patch within a once uniformly stratified fluid. In this case, no transmission occurs for incident waves with phase speed matching the speed of the flow within the shear layer. However, a transmission spike occurs if the incident waves are resonant with interfacial waves that flank the shear.

RÉSUMÉ *[Traduit par la rédaction] Nous examinons la transmission des ondes de gravité internes à travers un fluide stratifié de façon non uniforme dont le cisaillement de fond varie verticalement. Pour quantifier la transmission des ondes, nous montrons que la mesure appropriée est le rapport du flux transmis au flux incident de pseudoénergie, T. Nous dérivons une prévision analytique de T pour la transmission des ondes à travers un écoulement cisaillé linéairement par morceaux dans deux cas. Dans chaque cas, le fluide est non stratifié dans toute l'épaisseur du cisaillement et uniformément stratifié ailleurs.*

Dans l'une des études, le profil de densité est continu. Un tel état de base est instable mais avec un taux de croissance devenant très faible à mesure que le nombre de Richardson, Ri, devient grand. À la limite d'un nombre de Richardson infiniment grand (pas de cisaillement), nous retrouvons la prévision de formation d'un tunnel de Sutherland et Yewchuk (2004). Quand le cisaillement est faible, les ondes incidentes peuvent être faiblement transmises, même si la vitesse de phase correspond à la vitesse de l'écoulement à l'intérieur de la couche de cisaillement (un niveau critique). Cependant, il n'y a aucune transmission quand la vitesse de phase des ondes incidentes correspond exactement à la vitesse de l'écoulement sur le flanc opposé du cisaillement. Quand le cisaillement est fort, avec Ri ≃ 1, il se produit un maximum de transmission là où le nombre d'ondes et la fréquence incidents sont proches, mais différents, de ceux qui caractérisent les modes instables.

Dans une deuxième étude, le profil de densité de fond est discontinu et représentatif d'une parcelle bien mélangée dans un fluide qui était auparavant uniformément stratifié. Dans ce cas, il n'y a pas de transmission pour les ondes incidentes dont la vitesse de phase correspond à la vitesse de l'écoulement dans la couche de cisaillement. Cependant, un maximum de transmission se produit si les ondes incidentes entrent en résonance avec les ondes d'interface se propageant sur le flanc du cisaillement.

1 Introduction

Internal gravity waves propagate through density stratified fluids with a frequency no larger than the buoyancy frequency, N, which under the Boussinesq approximation is defined by $N^2 = -(g/\rho_0)\, d\overline{\rho}/dz$. Here g is the gravitational acceleration, ρ_0 is a characteristic density, and $\overline{\rho}$ is the background density profile which is assumed to decrease monotonically

*Corresponding author's e-mail: Bruce.Sutherland@ualberta.ca

with height so that the fluid is stably stratified. Provided that the stratification and background horizontal flow, $\overline{U}$, are steady and independent of x, the absolute wave frequency, ω, and horizontal wavenumber, k, of internal waves remain constant as waves propagate. However, the relative (or 'Doppler-shifted') frequency,

$$\overline{\Omega}(z) \equiv \omega - k\overline{U}(z), \tag{1}$$

does change as waves move vertically and this, together with variations in the background stratification, essentially determines where waves break or reflect.

Simple heuristics based on ray theory (an application of Wentzel-Kramers-Brillouin (WKB) theory) state that small-amplitude waves reflect from a height, z_r (a reflection level), where $\overline{\Omega} = N$ and they asymptotically approach a height, z_c (a critical level), where $\overline{\Omega} = 0$. These heuristics are based on a scale separation that assumes that the vertical scale of variations of the background is large compared to the vertical wavelength of waves. This paper shows that when this scale separation is reversed, waves can indeed transmit across reflection and critical levels. The circumstance, being analogous to electron tunnelling in quantum mechanics, is referred to here as 'internal wave tunnelling'.

Internal wave tunnelling between two ducts in the ocean has previously been described theoretically by Eckart (1961), who considered resonant energy transfer between different vertical modes of the main and seasonal thermocline in the ocean. The atmospheric counterpart to Eckart resonance was described by Fritts and Yuan (1989) who additionally considered the effects of Doppler-shifting winds. This work usefully describes the two-way periodic energy transfer between ducts by low-order modes, however, it cannot describe one-way tunnelling of small vertical-scale internal waves from one highly stratified region to another.

Unidirectional tunnelling was examined by Lindzen and Tung (1976), who studied the reflection and over-reflection of atmospheric internal gravity waves. Their study was restricted to low-order mesoscale modes and so filtered non-hydrostatic waves with frequencies close to the buoyancy frequency. This work was continued by Wang and Lin (1999) who examined more general background velocity and density profiles.

An analytic theory for non-hydrostatic internal wave tunnelling through a weakly stratified fluid layer was derived by Sutherland and Yewchuk (2004). In particular they examined internal wave tunnelling through what they termed an "N^2-barrier', which consisted of a continuously varying background density profile in three distinct layers. The outer two layers were uniformly stratified with buoyancy frequency N_0 while the inner layer had uniform density and thus a buoyancy frequency of zero, seen in Fig. 1a. Tunnelling through an N^2-barrier can be viewed as an idealization of several large-scale geophysical flows. In the atmosphere it is representative of waves tunnelling from the stratosphere, through an evanescent region in the mesosphere, to the ionosphere, whereas, in the equatorial ocean it could idealize waves tunnelling from the turbulent surface layer, through a well-mixed patch in the thermocline, to the deep ocean. Defining the transmission coefficient as the ratio of transmitted to incident energy they found, in particular, that the maximum transmission across an N^2-barrier occurs for waves having frequency $\omega = N_0/\sqrt{2}$. They also studied tunnelling through a 'mixed-N^2' profile in which stratification was the same as in the N^2-barrier case except that it exhibited discontinuous density jumps on either flank of the unstratified region, seen in Fig. 1b. This circumstance was representative of a mixed layer caused by local mixing within an initially uniformly stratified fluid. They found that waves could transmit more effectively than through an N^2-barrier and that a transmission spike occurred when the vertically propagating waves interacted resonantly with interfacial waves on either flank of the shear layer.

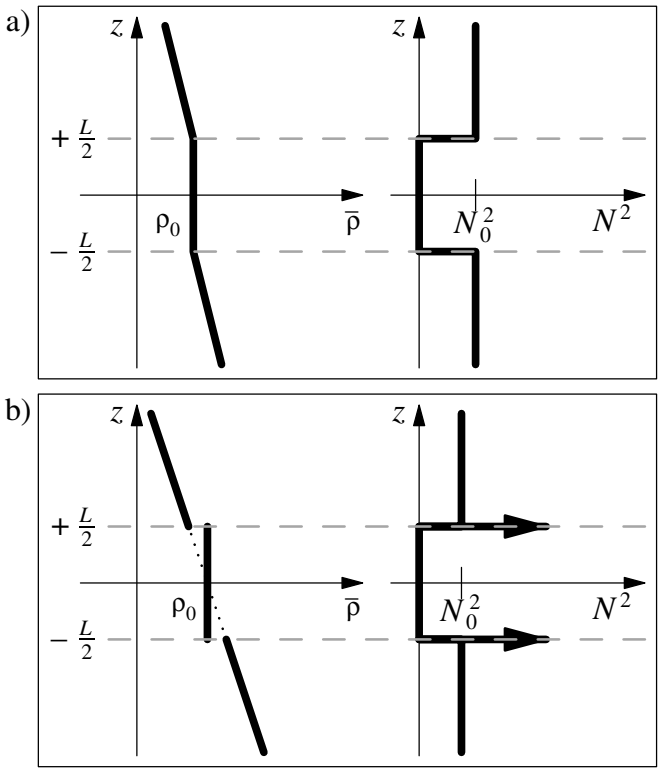

Fig. 1 Background density (left) and squared buoyancy frequency (right) defined for a) an 'N^2-barrier'and b) a 'mixed-N^2' profile.

In this paper, the work of Sutherland and Yewchuk (2004) is extended to include the effects of a shear layer coinciding with an unstratified region. The addition of shear makes the mixed-N^2 case in particular, more closely resemble a mixed layer because the presence of shear may act as a source of the local mixing that results in the uniform density region.

In Section 2 of this paper we provide the theoretical preliminaries for the tunnelling calculation. In particular, we define a transmission coefficient to be the ratio of the vertical flux of transmitted to incident pseudoenergy. This differs from the traditional definition of a ratio of energies because the presence of shear means that wave energy is no longer

conserved (Eliassen and Palm, 1961; Bretherton and Garrett, 1969; Andrews and Mcintyre, 1976). In Section 3 we examine the stability of the piecewise-linear shear layer as a function of the bulk Richardson number, Ri, for the N^2-barrier case. The point of this calculation is to show that the unstable flow has such small growth rates for large Ri that it is reasonable to consider tunnelling across the flow as if it were stable. It also provides a connection between our work and the over-reflection study of Lindzen and Tung (1976). In Section 4 we plot the analytically predicted transmission coefficient for waves across the piecewise-linear shear layer in both the N^2-barrier and mixed-N^2 cases. Conclusions are given in Section 5.

2 Background theory

a *Wave Structure*

We restrict our study to small-amplitude two-dimensional disturbances in a non-rotating, inviscid, Boussinesq fluid. The perturbation streamfunction associated with disturbances having horizontal wavenumber, k, and (absolute) frequency, ω, is $\psi = \phi(z)\exp[i(kx - \omega t)]$, where the streamfunction amplitude, ϕ, satisfies the Taylor-Goldstein equation

$$\phi'' + k^2\left(\frac{N^2}{\bar{\Omega}^2} + \frac{\bar{U}''}{k\bar{\Omega}} - 1\right)\phi = 0. \tag{2}$$

In this formula $\bar{\Omega}$ is the relative frequency given by Eq. (1). If the coefficient of ϕ in Eq. (2) is constant for all z in the domain, solutions are either exponential or sinusoidal functions. This occurs if N^2 is piecewise-constant and $\bar{U}$ is piecewise-linear such that N^2 is zero where $\bar{U}$ is variable.

A complete solution for ϕ is found by matching the functions determined over each piecewise-linear segment using conditions that require the vertical velocity and pressure to be continuous. This is done by requiring the continuity of $\phi/\bar{\Omega}$ and $\bar{\rho}\,(\bar{\Omega}\phi' + k\bar{U}'\,\phi - gk^2\phi/\bar{\Omega})$ (Drazin and Reid, 1981). For a fluid with continuous background horizontal flow, $\bar{U}$, the first of these matching conditions reduces to

$$\Delta\left[\phi(z)\right] = 0 \tag{3}$$

where the Δ operator is defined by

$$\Delta\left[\phi(z)\right] \equiv \lim_{z\to z_*^+}\phi(z) - \lim_{z\to z_*^-}\phi(z).$$

This condition, Eq. (3), is applied at every z_* where $\bar{U}'$ or $\bar{\rho}$ is discontinuous. Strictly speaking, these interfaces will be deformed by the presence of the wave; however, since the wave amplitudes are small ($|Ak| \ll 1$), the matching conditions are applied at constant elevations. Under the Boussinesq approximation the second matching condition reduces to

$$\Delta\left[\rho_0\left(\bar{\Omega}\phi' + k\bar{U}'\phi\right) - \bar{\rho}\,\frac{gk^2}{\bar{\Omega}}\phi\right] = 0. \tag{4}$$

If additionally the background density profile, $\bar{\rho}$, is continuous, this condition together with Eq. (3) further reduces to

$$\Delta\left[\bar{\Omega}\phi' + k\bar{U}'\phi\right] = 0. \tag{5}$$

We also require boundary conditions suitable for a vertically unbounded domain. In the stability problem, this amounts to requiring bounded solutions such that internal waves, if they occur in the far field, propagate outward from the unstable region. The resulting equations form an eigenvalue problem in which the eigenvalue specifies the frequency and possibly the growth rate as a function of the horizontal wavenumber. The eigenfunction specifies the structure of the disturbance whose amplitude is arbitrary, though small.

In the tunnelling problem, we specify the amplitude, frequency, and horizontal wavelength of an incident wave that propagates inward from the far field and the boundary conditions require that, if waves transmit into the far field on the opposite side of the domain, then they must propagate outward. This is not an eigenvalue problem; both ω and k are independently specified. The resulting equations allow us to determine how the amplitude of the transmitted waves depends upon the amplitude of the incident waves.

b *Transmission Coefficients*

In the tunnelling problem the amplitude of a transmitted wave can be found in terms of an incident wave amplitude, frequency, and wavelength as well as any parameters associated with the problem, such as Richardson number.

When no shear is present and the N is the same for transmitted waves as for incident waves we define a transmission coefficient,

$$T \equiv \left|\frac{A_T}{A_I}\right|^2, \tag{6}$$

as the square magnitude of the ratio of transmitted to incident wave amplitude. This may be interpreted as the ratio of outgoing to incoming wave energy, E, defined in the classical sense of the mean kinetic and potential energy associated with the fluid parcels over one wavelength.

This was done by Sutherland and Yewchuk (2004), who in part studied the partial transmission and reflection of waves across a piecewise-constant N^2-barrier of depth L prescribed by

$$N^2(z) = \begin{cases} N_0^2 & |z| > \dfrac{L}{2} \\ 0 & |z| \le \dfrac{L}{2} \end{cases} \tag{7}$$

which corresponds to a continuous background density profile of

$$\bar{\rho}(z) = \rho_0\begin{cases} 1 - \dfrac{N_0^2}{g}\left(z - \dfrac{L}{2}\right) & z > \dfrac{L}{2} \\ 1 & |z| < \dfrac{L}{2} \\ 1 - \dfrac{N_0^2}{g}\left(z - \dfrac{L}{2}\right) & z < -\dfrac{L}{2} \end{cases} \tag{8}$$

as seen in Fig. 1a. Defining $\Theta \equiv \cos^{-1}(\omega/N_0)$, they found the transmission coefficient to be

$$T = \left[1 + \left(\frac{\sinh(kL)}{\sin 2\Theta}\right)^2\right]^{-1}. \quad (9)$$

They also studied the partial transmission and reflection of waves across a piecewise-constant mixed-N^2 profile where the background density is prescribed as

$$\bar{\rho}(z) = \rho_0 \begin{cases} 1 - \dfrac{N_0^2}{g} z & |z| > \dfrac{L}{2} \\ 1 & |z| \le \dfrac{L}{2} \end{cases}. \quad (10)$$

Here the buoyancy frequency is the same as Eq. (7) except that $N^2 \to \infty$ at $z = \pm L/2$, seen in Fig. 1b. The corresponding transmission coefficient was determined to be

$$T = \left[1 + \left(\frac{\sinh(kL)}{\sin 2\Theta}\right)^2 \left(1 + \frac{(kL)^2}{4\cos^2\Theta} - kL\coth(kL)\right)^2\right]^{-1}. \quad (11)$$

When shear is present in the background flow the transmission coefficient for the tunnelling problem cannot be defined as a ratio of wave energies. In shear flow, wave energy is not a conserved quantity but can be created or destroyed through the interaction of the Reynolds stress with the background shear. What is conserved for small-amplitude waves is the wave action, $\mathcal{A} \equiv E/\bar{\Omega}$, defined by the ratio of the wave energy to the relative frequency (Eliassen and Palm, 1961; Andrews and Mcintyre, 1976). More generally, the pseudoenergy is conserved which, in the small-amplitude limit, is the wave energy multiplied by $\omega/\bar{\Omega}$ (Andrews and Mcintyre, 1978; Scinocca and Shepherd, 1992). This is proportional to the wave action, but has the same units as energy. Since pseudoenergy is a conserved quantity, to classify the transmission of waves across a non-uniformly stratified shear flow, an appropriate definition of the transmission coefficient is the ratio of the transmitted to incident vertical flux of pseudoenergy. In the small-amplitude limit, the vertical flux of pseudoenergy is $c_{gz}E\omega/\bar{\Omega}$, the vertical group velocity multiplied by the pseudoenergy. After cancellation, the transmission coefficient is therefore defined as the ratio of transmitted to incident squared wave amplitude multiplied by the ratio of transmitted to incident vertical wavenumber,

$$T \equiv \left|\frac{A_T}{A_I}\right|^2 \frac{m_T}{m_I}. \quad (12)$$

If there is no background shear the vertical wavenumbers of transmitted and incident waves are identical and thus this definition of the transmission coefficient is equivalent to the ratio of transmitted to incident wave energy.

3 Stability problem

Before performing the tunnelling calculation we first consider the stability of the prescribed stratification and shear layer, with respect to a bulk Richardson number, defined by

$$\mathsf{Ri} = \left(\frac{N_0 L}{U_0}\right)^2. \quad (13)$$

Here N_0, U_0, and L are the characteristic buoyancy frequency, flow speed, and length scale, respectively, associated with the problem. A necessary (but not sufficient) condition for instability is that $\mathsf{Ri} < 1/4$ in which the gradient Richardson number is defined as $\mathsf{Ri}_g = N^2(z)/(\bar{U}')^2(z)$. The profiles we consider have $\mathsf{Ri}_g = 0$ in the shear region meaning that instability is possible. The purpose of this section is to determine how the stability of our prescribed stratification and background flow depend on the bulk Richardson number, Ri.

We consider a non-uniformly stratified shear layer of depth L in which N^2 is prescribed by Eq. (7) and the background flow by

$$\bar{U}(z) = \begin{cases} \dfrac{1}{2}U_0 & z > \dfrac{L}{2}, \\ \dfrac{U_0 z}{L} & |z| < \dfrac{L}{2}, \\ -\dfrac{1}{2}U_0 & z < -\dfrac{L}{2}. \end{cases} \quad (14)$$

These are illustrated in Fig. 2a.

The solutions to the governing equation, Eq. (2), for these profiles take the form

$$\phi(z) = \begin{cases} A_2 e^{im_- z} & z > \dfrac{L}{2} \\ B_1 e^{kz} + B_2 e^{-kz} & |z| < \dfrac{L}{2} \\ A_1 e^{im_+ z} & z < -\dfrac{L}{2}, \end{cases} \quad (15)$$

in which

$$m_\pm = \pm k\left[\frac{N_0^2}{\Omega_\pm^2} - 1\right]^{1/2}, \quad (16)$$

and

$$\Omega_\pm = \omega \pm kU_0/2. \quad (17)$$

If $|\Omega_\pm| \le N_0$, the vertical wave number, $m_\pm$, is defined so that waves propagate away from the shear layer. For complex $m_\pm$, branch cuts are taken so that disturbances decay exponentially away from the shear layer. Applying matching conditions Eq. (3) and Eq. (5) at $z = \pm L/2$, gives an eigenvalue problem

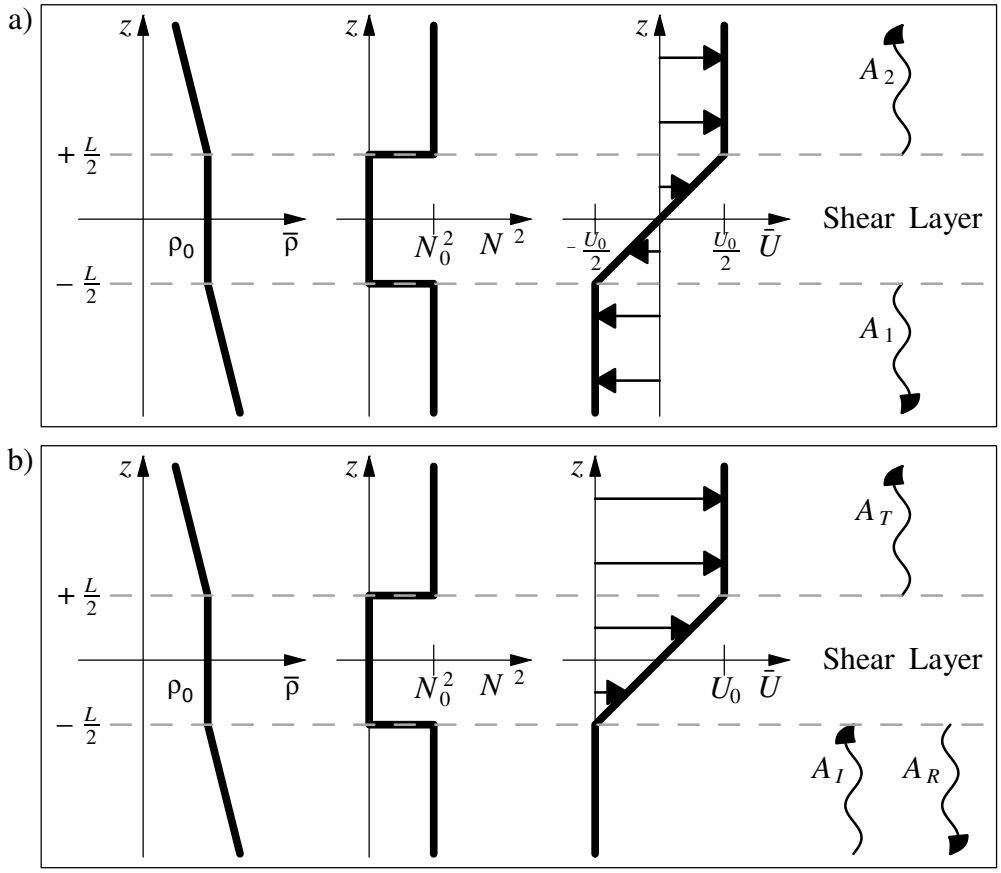

Fig. 2 Background density (left), squared buoyancy frequency (middle), and velocity (right) profiles defined for a) the stability calculation and b) the tunnelling calculation. In a) A_1, and A_2 are the amplitudes of the emitted disturbances. In b) A_I, A_R, A_T are the amplitudes of the incident, reflected, and transmitted waves respectively.

that predicts frequency as a function of wavenumber, k, through a cubic polynomial in ω^2:

$$\tilde{\omega}^6 + C_4\tilde{\omega}^4 + C_2\tilde{\omega}^2 + C_0 = 0. \tag{18}$$

Here the formula is given in non-dimensional form with $\tilde{\omega} = \omega L/U_0$. The coefficients $C_i(\tilde{k};\mathrm{Ri})$ for $i = 0, 2, 4$ are functions of the non-dimensional horizontal wavenumber $\tilde{k} = kL$ and the bulk Richardson number, Ri. These coefficients are explicitly given in the Appendix.

Of the three roots of Eq. (18) (in $\tilde{\omega}^2$), only one is physical and the others are spurious. The appropriate root is determined by taking the limit as $N_0 \to 0$ and selecting that which corresponds to the classic result for unstratified shear flow (Drazin and Reid, 1981):

$$\tilde{\omega}^2 = \left[\left(\tilde{k}-1\right)^2 - e^{-2\tilde{k}}\right]/4. \tag{19}$$

The physical root, decomposed into its real and imaginary parts, is plotted in Fig. 3. The left panel shows that the system is unstable for every value of Ri. However, the instability occurs over a decreasing range of kL about $\mathrm{Ri} = kL - 1$ as Ri increases. The marginal stability curves are given by

$$\mathrm{Ri} = \left(\tilde{k}/2\right)^2 - \left[\left(\tilde{k}/2\right)\coth\left(\tilde{k}/2\right) - 1\right]^2 \tag{20}$$

and

$$\mathrm{Ri} = \left(\tilde{k}/2\right)^2 - \left[\left(\tilde{k}/2\right)\tanh\left(\tilde{k}/2\right) - 1\right]^2 \tag{21}$$

when $\mathrm{Ri} \geq 1$.

From the right-hand panel we notice that when a wave is unstable the frequency of the wave, and thus the wave speed, is exactly zero: the speed matches the background flow speed at the midpoint of the shear. We also notice that the growth rate, $\tilde{\omega}_i$, of the instability decreases as Ri increases. So, although the gradient Richardson number, Ri_g, is zero in the shear region, instability is weak if the bulk Richardson number, Ri, is large enough.

We have not explicitly performed the stability calculation for the mixed-N^2 profile in which $\bar{\rho}$ is given by Eq. (10) rather than Eq. (8). The matching conditions make finding an analytic solution significantly more complex in this circumstance. However, we expect that the density jumps at $z = \pm L/2$ will further serve to stabilize the flow.

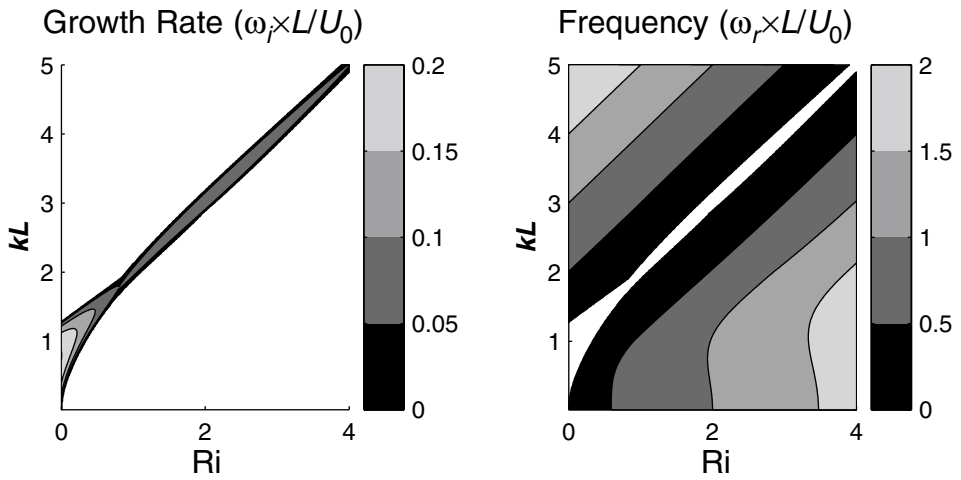

Fig. 3 The non-dimensional growth rate ($\tilde{\omega}_i = \omega_i L/U_0$) and frequency ($\tilde{\omega}_r = \omega_r L/U_0$) defined by the physical root of Eq. (18).

4 Tunnelling solution

In Section 3 we found that for large enough Ri, the instability growth rate of a piecewise-linear shear layer is smaller than the time for wave propagation across a coinciding uniform density region. We now consider internal wave tunnelling across a piecewise-linear shear layer in this large Ri limit. To this end we assume that the prescribed background flow and density profiles are steady and study the circumstance of an internal gravity wave impinging from below upon an unstratified layer.

For conceptual convenience, we now shift to a frame of reference moving with the speed of the flow below $z = -L/2$. The shear flow profile is given by

$$\bar{U}(z) = \begin{cases} U_o & z > \dfrac{L}{2} \\ \dfrac{U_0}{L}\left(z + \dfrac{L}{2}\right) & |z| < \dfrac{L}{2} \\ 0 & z < -\dfrac{L}{2} \end{cases}. \tag{22}$$

For this choice of velocity profile the relative frequency of an internal wave below $z = -L/2$ is the same as its absolute frequency, ω. Above $z = +L/2$ the relative frequency is given by

$$\Omega \equiv \omega - kU_0. \tag{23}$$

a *Transmission Across an 'N^2 Barrier'*

We begin by examining internal wave tunnelling across an N^2-barrier with N^2 given by Eq. (7) and the shear flow given by Eq. (22) as plotted in Fig. 2b. We suppose that a wave with given k, ω, and streamfunction amplitude, A_I, is incident upon the shear region from below. The phase speed of this wave is $c \equiv \omega/k$. Without loss of generality, we only allow positive values for ω so that the horizontal direction of wave propagation is entirely determined by the sign of k.

Similar to Eq. (15), solutions to the Taylor-Goldstein equation, Eq. (2), in each piecewise-linear region take the form

$$\phi(z) = \begin{cases} A_T e^{-im_T z} & z > \dfrac{L}{2} \\ B_1 e^{kz} + B_2 e^{-kz} & |z| < \dfrac{L}{2} \\ A_I e^{-im_I z} + A_R e^{im_I z} & z < -\dfrac{L}{2} \end{cases} \tag{24}$$

in which

$$m_I \equiv |k \tan\Theta| \text{ and } m_T \equiv |k \tan\Phi| \tag{25}$$

are vertical wavenumbers for the incident and transmitted waves, respectively. We have defined

$$\Theta \equiv \cos^{-1}\left(\frac{\omega}{N_0}\right) \text{and } \Phi \equiv \cos^{-1}\left(\frac{\Omega}{N_0}\right). \tag{26}$$

These represent the angle between lines of constant phase and the vertical for incident and transmitted waves respectively. Notice that φ includes solutions for both incident and reflected waves below $z = -L/2$. Applying the matching conditions, Eq. (3) and Eq. (5), at $z = \pm L/2$ gives a system of four equations and five unknowns.

Solving these for the transmitted amplitude, A_T, in terms of the incident amplitude, A_I, gives a transmission coefficient, T, defined as the ratio of transmitted to incident pseudoenergy flux given by

$$T = \left|\frac{A_T}{A_I}\right|^2 \left|\frac{\tan\Phi}{\tan\Theta}\right|, \tag{27}$$

in which we have used Eq. (12) with the relationship between vertical wavenumber and propagation angle, Eq. (25).

Likewise we may define the reflection coefficient, R, to be the magnitude of the reflected to incident pseudoenergy flux. In this case the ratio of vertical wavenumbers cancels and we find $R = |A_R|^2/|A_I|^2$. Tests show that the relationship $T + R \equiv 1$ holds, as expected.

After extensive algebraic manipulation the transmission coefficient is found to be

$$T^{-1} = 1 + \frac{\left\{ \begin{array}{l} \sinh(kL) + \\ \frac{1}{\mathsf{Ri}}\left[\sinh\left(kL\right) - kL\cosh\left(kL\right)\right] \end{array} \right\}^2 + \alpha^2 - \frac{1}{\mathsf{Ri}}\beta^2}{\left|\sin 2\Theta \sin 2\Phi\right|}, \quad (28)$$

in which

$$\alpha = \sin\left(\Theta \mp \Phi\right) \quad (29)$$

and

$$\beta = \left(\cos\Theta + \cos\Phi\right)\sinh\left(kL\right). \quad (30)$$

The angles in Eq. (29) are subtracted if $\tan\Theta$ and $\tan\Phi$ are of the same sign and they are summed otherwise. Together with Eq. (23) and Eq. (26), this reduces to Eq. (9) in the limit as $\mathsf{Ri} \to \infty$ (corresponding to $U_0 \to 0$ and $\Phi \to \Theta$ at fixed L). For any finite Ri (in which U_0/L is fixed) we find $T \to 1$ for fixed k as $L \to 0$. In this instance the background is reduced to constant N^2 with vanishingly small shear. Note that for finite Ri the numerator can be negative, corresponding to $T > 1$. This corresponds to waves acting in near resonance with unstable modes so that transmitted waves can draw energy from both the incident waves and the mean flow. This occurs only for $\mathsf{Ri} \ll 1$ in which case the mean flow is strongly unstable.

Contour plots of T as a function of kL and ω/N_0 in four cases, each with different values of Ri, are given in Fig. 4a. In the upper-left panel $\mathsf{Ri} = 10^6$ is chosen to be so large that the shear flow is effectively non-existent: $U_0 \simeq 0$. As expected in this limit, T approaches the value found by Sutherland and Yewchuk (2004).

For smaller Ri, Doppler-shifting by the shear flow plays an increasingly significant role. As required by Eq. (24), there is no transmission of waves if the magnitude of the relative frequency of waves above $z = +L/2$ exceeds N_0. For non-trivial solutions, this forces the absolute frequency and wavelength of the incident waves to lie within a parameter regime shown schematically in Fig. 4b. The allowable frequencies and wavelengths are bounded by the solid lines $\omega = 0$, $\omega = N_0$ and the dash-dotted lines $\Omega = \pm N_0$. This bounded region can be further separated into two subregimes separated by a dashed line which denotes waves whose relative frequency is $\Omega = 0$. Below this line incident waves propagate faster than U_0 or in the opposite direction from the flow above $z = +L/2$ (i.e., $c < 0$) and therefore they do not encounter a critical level. Above the dashed line, waves propagate with phase speed $0 < c < U_0$ and thus encounter a critical level within the shear layer.

From Fig. 4a we find that, for all Ri, near-perfect transmission occurs for waves with $|kL| \ll 1$. For the smaller values of Ri, the transmission coefficient is exactly zero along the dashed line where the horizontal phase speed of the incident waves matches the flow speed above the shear layer, U_0. Such behaviour may be anticipated from the heuristic prediction that waves cannot penetrate through a critical level. Surprisingly, however, for $\mathsf{Ri} = 1$ and 3 we see transmission for internal waves which encounter a critical level within the shear layer. Incident waves are able to cross the critical level because $N^2 = 0$ in the shear region, and so all disturbances are evanescent, not wave-like there. We find nearly perfect transmission for waves with $kL \lesssim 2$ and $\omega \lesssim N_0$ if $\mathsf{Ri} = 1$. To examine the transmission spike, we plot the transmission contours for $\mathsf{Ri} = 1$ as a function of the incident phase speed and wavenumber in Fig. 4c. We find that the transmission spike occurs for waves with a phase speed equal to the midpoint of the shear ($c = U_0/2$). Waves within the transmission spike have wavenumbers and frequencies that are nearly resonant with those of unstable modes. Indeed, Fig. 3 shows that unstable modes occur when $kL \simeq 2.08$. The full range of unstable modes is indicated in Fig. 4c by the error-bar and lies outside, but close to, the allowable parameter range for internal waves. Although we see a large transmission spike for propagating internal waves, disturbances which lie in the range of unstable modes are evanescent at all levels in the flow for $\mathsf{Ri} = 1$.

For still smaller Ri, the parameter range for unstable modes increases to lie within the allowable range for propagating internal waves. In this case, we expect to see transmission coefficients exceeding unity, meaning that the incident waves draw energy from the mean flow and so transmit across the shear at larger amplitude. In the absence of incident waves, this is the process of 'over-reflection' (ie., Lindzen and Tung (1976)). We have not examined this circumstance in detail because the timescale for instability compared with the time for waves to cross the shear layer is so small that it is hard to imagine a realistic circumstance in which incident waves might encounter the unstable shear layer before it develops non-linearly.

b *Transmission Across a Locally Mixed Region*

In the circumstance considered in Section 4a, $\bar{\rho}$ varies continuously, even though its slope is discontinuous at $z = \pm L/2$. More realistically, localized mixed regions within a stratified fluid are better represented by the discontinuous density profile given by Eq. (10), seen in Fig. 1b. Thus we now examine internal wave tunnelling across such a mixed-N^2 profile.

We proceed exactly as in the preceding section to find solutions to Eq. (2) given by Eq. (24). The difference is that we must now apply the matching conditions, Eq. (3) and Eq. (4), for discontinuous density profiles to determine the transmitted amplitude in terms of the incident wave amplitude. The transmission coefficient is defined as in Eq. (27) and can be determined as before. We do not explicitly give the equation here because of its complexity, but we do plot contours of the transmission coefficient in Fig. 5.

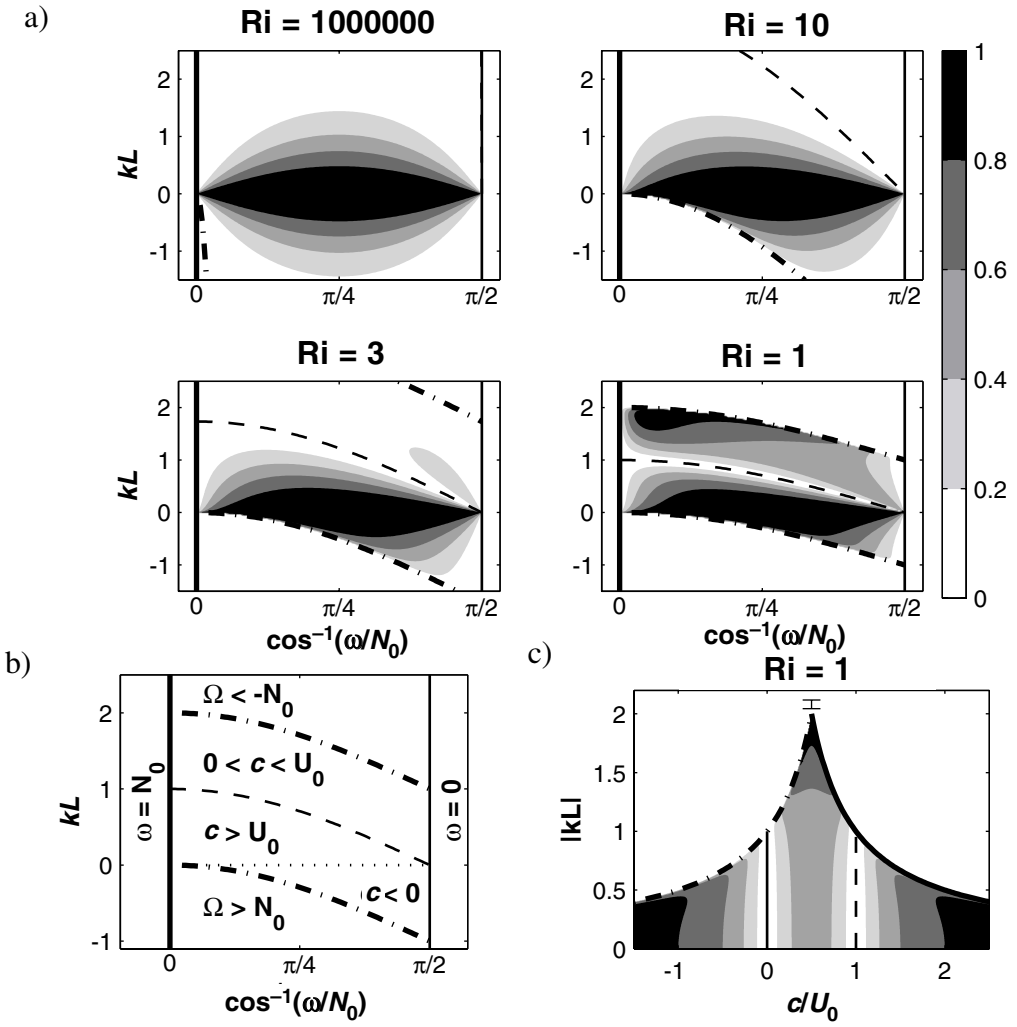

Fig. 4 a) Contour plots of the transmission coefficient, T, for internal gravity waves traversing an N^2-barrier as a function of frequency and wavenumber for several values of the bulk Richardson number, Ri, as indicated. b) Schematic formulae defining the bounding lines in the contour plots. Wave transmission is bounded between the solid and dash-dotted lines where the relative frequency of incident and transmitted waves respectively equal the buoyancy frequency. The dashed line separates waves that encounter a critical level and those that do not. c) Values of the transmission coefficient as a function of wavenumber and phase speed for Ri = 1.

In these plots the lines that create a bounding box and the dashed lines are defined exactly as in the previous section. In the case of negligibly small shear (Ri = 10^6) transmission is the same as that found by Sutherland and Yewchuk (2004). One obvious difference between the N^2-barrier and mixed-N^2 case is the appearance of a transmission spike for waves with $\omega \lesssim N_0$ and $kL \simeq 2.4$. This occurs due to coupling of the propagating internal gravity waves and interfacial waves which are situated at the density jumps above and below the shear layer.

For smaller Ri, this transmission spike remains as the dominant feature causing transmission to be much greater than in the N^2-barrier case. In fact, transmission is nearly perfect for almost half the allowable range of frequencies and wavenumbers.

For small Ri, the most notable difference between transmission in the N^2-barrier and mixed-N^2 case is the lack of transmission above the dashed line where incident waves encounter a critical level. The presence of density jumps bounding a shear layer apparently inhibits transmission across critical levels in uniform-density fluid.

5 Conclusions

Using pseudoenergy flux to quantify transmission coefficients, we have derived an analytic prediction for internal wave tunnelling across a uniformly mixed shear layer surrounded by a stratified fluid. For transmission to occur, the magnitude of the Doppler-shifted frequency of the transmitted waves must be less than the buoyancy frequency and the phase speed cannot match the flow speed beyond the shear region. For weak shear, maximum transmission occurs for waves with $\omega = N_0/\sqrt{2}$ (equal horizontal and vertical wavenumbers). For stronger shear, waves can transmit across a critical level (where the wave speed matches the

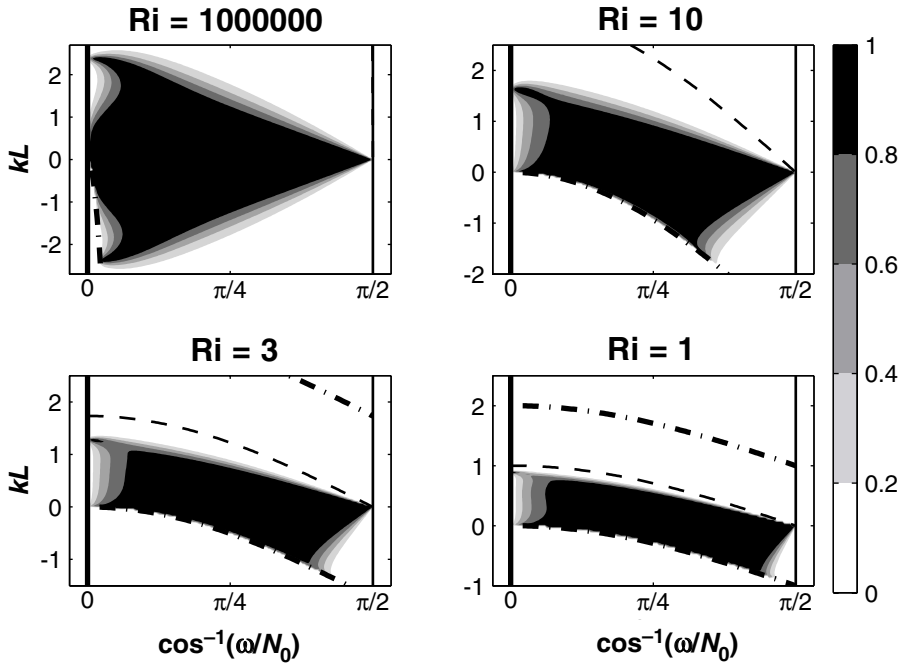

Fig. 5 As in Fig. 4a, but for internal gravity waves traversing a mixed-N^2 profile.

background flow speed) if the buoyancy frequency is zero at the critical level. The presence of density jumps in the background profile serves to enhance transmission when no critical level is reached, but inhibits transmission across critical levels.

Future work will examine the transmission and reflection of internal gravity waves for geophysically relevant background profiles of N^2 and $\overline{U}$. In particular we will study internal waves propagating downward through the equatorial undercurrent and include anelastic effects (non-Boussinesq) in order to examine wave transmission across the mesosphere into the upper atmosphere.

Acknowledgments

This research was supported by the Canadian Foundation for Climate and Atmospheric Science (CFCAS).

Appendix

In Section 3 we found the linear stability of the N^2-barrier in terms of the frequency as a function of wavenumber, k, and the bulk Richardson number, Ri. The linear stability equation (Eq. (18)), is

$$\tilde{\omega}^6 + C_4\tilde{\omega}^4 + C_2\tilde{\omega}^2 + C_0 = 0.$$

where $\tilde{\omega} = \omega\, L/U_0$. The coefficients $C_i(kL;\mathrm{Ri})$ are given here for completeness.

$$C_4 \equiv \sinh^2(kL) - \left[\mathrm{Ri} + 2\left(\frac{kL}{2}\right)^2\right] - \left[\frac{\mathrm{Ri}\Gamma}{2\sinh(kL)}\right]^2,$$

$$C_2 \equiv \left(\frac{kL}{2}\right)^4 - \mathrm{Ri}\left(\frac{kL}{2}\right)^2 - \frac{1}{2}\mathrm{Ri}^2\Gamma^2 + \left(\frac{kL}{2}\right)^2 \frac{\mathrm{Ri}^2}{\sinh^2(kL)} + \left[\mathrm{Ri} + 2\left(\frac{kL}{2}\right)^2\right]\left[\frac{\mathrm{Ri}\Gamma}{2\sinh(kL)}\right]^2,$$

and

$$C_0 \equiv -\left[\left(\frac{kL}{2}\right)^4 - \mathrm{Ri}\left(\frac{kL}{2}\right)^2 - \frac{1}{4}\mathrm{Ri}^2\Gamma^2\right]\left[\frac{\mathrm{Ri}\Gamma}{2\sinh(kL)}\right]^2$$

in which

$$\Gamma \equiv \sinh(kL) + \tfrac{1}{\mathrm{Ri}}\left[\sinh(kL) - kL\cosh(kL)\right].$$

References

ANDREWS, D. G. and M. E. MCINTYRE. 1976. Planetary waves in horizontal and vertical shear: The generalized Eliassen-Palm relation and the mean flow acceleration. *J. Atmos. Sci.* **33**: 2031–2048.

——— and ———. 1978. On wave action and its relatives. *J. Fluid Mech.* **89**: 647–664.

BRETHERTON, F. P. and C. J. R. GARRETT. 1969. Wavetrains in inhomogeneous moving media. *Proc. Roy. Soc. A.* **302**: 529–554.

DRAZIN, P. G. and W. H. REID. 1981. *Hydrodynamic Stability*. Cambridge University Press, Cambridge, England. 525 pp.

ECKART, C. 1961. Internal waves in the ocean. *Phys. Fluids.* **4**: 791–799.

ELIASSEN, A. and E. PALM. 1961. On the transfer of energy in stationary mountain waves. *Geofys. Publ.* **22**: 1–23.

FRITTS, D. C. and L. YUAN. 1989. An analysis of gravity wave ducting in the atmosphere: Eckart's resonances in thermal and Doppler ducts. *J. Geophys. Res.* **94**(D15): 18455–18466.

LINDZEN, R. S. and K.-K. TUNG. 1976. Banded convective activity and ducted gravity waves. *Mon. Weather Rev.* **104**: 1602–1617.

SCINOCCA, J. F. and T. G. SHEPHERD. 1992. Nonlinear wave-activity conservation laws and Hamiltonian structure for the two-dimensional anelastic equations. *J. Atmos. Sci.* **49**: 5–27.

SUTHERLAND, B. R. and K. YEWCHUK. 2004. Internal wave tunnelling. *J. Fluid Mech.* **511**: 125–134.

WANG, T. A. and Y. L. LIN. 1999. Wave ducting in a statified shear flow over a two-dimensional mountain. part 1: General linear criteria. *J. Atmos. Sci.* **56**: 412–436.